

PAPER • OPEN ACCESS

## A charged particle veto detector for kaonic deuterium measurements at DAΦNE

To cite this article: M Tüchler *et al* 2018 *J. Phys.: Conf. Ser.* **1138** 012012

View the [article online](#) for updates and enhancements.



**IOP | ebooks™**

Bringing you innovative digital publishing with leading voices to create your essential collection of books in STEM research.

Start exploring the collection - download the first chapter of every title for free.

## A charged particle veto detector for kaonic deuterium measurements at DAΦNE

M Tüchler<sup>1</sup>, J Zmeskal<sup>1,2</sup>, A Amirkhani<sup>3</sup>, M Bazzi<sup>2</sup>, G Bellotti<sup>3</sup>,  
C Berucci<sup>1,2</sup>, D Bosnar<sup>4</sup>, A M Bragadireanu<sup>5</sup>, M Cargnelli<sup>1</sup>,  
C Curceanu<sup>2</sup>, A Dawood Butt<sup>3</sup>, R Del Grande<sup>2</sup>, L De Paolis<sup>2</sup>,  
L Fabbietti<sup>6</sup>, C Fiorini<sup>3</sup>, F Ghio<sup>2</sup>, C Guaraldo<sup>2</sup>, R S Hayano<sup>7</sup>,  
M Iliescu<sup>2</sup>, M Iwasaki<sup>7</sup>, P Levi Sandri<sup>2</sup>, J Marton<sup>1,2</sup>, M Miliucci<sup>2</sup>,  
P Moskal<sup>8</sup>, D Pietreanu<sup>2,5</sup>, K Piscicchia<sup>2,9</sup>, A Scordo<sup>2</sup>, H Shi<sup>2</sup>,  
M Silarski<sup>8</sup>, D Sirghi<sup>2,5</sup>, F Sirghi<sup>2,5</sup>, M Skurzok<sup>8</sup>, A Spallone<sup>2</sup>,  
O Vazquez Doce<sup>2,6</sup> and E Widmann<sup>1</sup>

<sup>1</sup> Stefan Meyer Institute for Subatomic Physics, Boltzmanngasse 3, 1090 Vienna, Austria

<sup>2</sup> INFN, Laboratori Nazionali di Frascati, Frascati (Roma), Italy

<sup>3</sup> Politecnico Milano, Dipartimento di Elettronica, Informazione e Bioingegneria and INFN Sezione di Milano, Milano, Italy

<sup>4</sup> Physics Department, University of Zagreb, Zagreb, Croatia

<sup>5</sup> Horia Hulubei National Institute of Physics and Nuclear Engineering (IFIN-HH), Magurele, Romania

<sup>6</sup> Excellence Cluster Universe, Technische Universität München, Garching, Germany

<sup>7</sup> University of Tokyo, Tokyo, Japan

<sup>8</sup> The M. Smoluchowski Institute of Physics, Jagiellonian University, Krakow, Poland

<sup>9</sup> Museo Storico della Fisica e Centro Studi e Ricerche "Enrico Fermi", Roma, Italy

E-mail: marlene.tuechler@oeaw.ac.at, johann.zmeskal@oeaw.ac.at

**Abstract.** The antikaon-nucleon interaction close to threshold provides crucial information on the interplay between spontaneous and explicit chiral symmetry breaking in low-energy QCD. In this context, the importance of kaonic deuterium x-ray spectroscopy has been well recognized, but no experimental results have yet been obtained due to the difficulty of the measurement. To measure the shift and width of the kaonic deuterium  $1s$  state with an accuracy of 30 eV and 75 eV, respectively, an apparatus is under construction at the Laboratori Nazionali di Frascati. A detailed Monte Carlo simulation has shown that an increase of the signal to background ratio by a factor of ten will be required compared to the successfully performed kaonic hydrogen measurement (SIDDHARTA). Three pillars are essential for the newly developed experimental apparatus: a large area x-ray detector system (consisting of Silicon Drift Detectors), a lightweight cryogenic target system and a veto system, consisting of an outer veto detector (Veto-1) for active shielding and an inner veto detector (Veto-2) for charged particle suppression. For both veto systems, an excellent time resolution is required to distinguish kaons stopping in gas from direct kaon stops in the entrance window or side wall of the target. First test measurements on the Veto-2 system were performed. An average time resolution of  $(54 \pm 2)$  ps and detection efficiencies of  $\sim 99\%$  were achieved.



## 1. Introduction

The SIDDHARTA-2 experiment (Silicon Drift Detector for Hadronic Atom Research by Timing Application), located at the DAΦNE collider in Frascati, Italy, aims to perform precision measurements on kaonic deuterium in the non-perturbative regime of quantum chromodynamics (QCD) with strangeness.

The kaon is captured in an atomic orbit with principal quantum number  $n \sim 25$  and cascades down. A shift  $\epsilon_{1s}$  and broadened width  $\Gamma_{1s}$  of the ground state are induced via the strong interaction which are obtained by measuring  $2p - 1s$  x-ray transitions [1]. The combination of the existing kaonic hydrogen results [2] with the deuterium measurements will allow for the extraction of the isospin-dependent ( $I = 0, 1$ ) antikaon-nucleon scattering lengths  $a_0$  and  $a_1$  and further constrain the theoretical description of the low-energy  $\bar{K}N$  interactions, e.g. chiral symmetry breaking [3, 4].

The experimental challenge of the proposed measurement is the very small kaonic deuterium x-ray yield and the high radiation environment of an accelerator. A profound knowledge of each possible background source is essential in order to control and to improve the signal to background ratio. Using the experience gained with SIDDHARTA, a detailed study of the background was performed, using the theoretical input for shift and width of the kaonic deuterium  $1s$  state and assumption for the x-ray yield [5, 6]. The Monte Carlo (MC) calculation using the GEANT4 framework (GEometry ANd Tracking) has been crucial to finalise the realisation of the experimental setup and to eventually prove the possibility to perform the kaonic deuterium experiment with a precision determination of the shift and width in the order of 30 and 75 eV, respectively.

The outcome of the detector developments and dedicated MC studies can be summarised in three main updates essential for a successful kaonic deuterium x-ray experiment:

- An improved x-ray detection system based on newly developed Silicon Drift Detectors (SDDs) with excellent timing capability (300 ns) and energy resolution ( $\approx 150$  eV), to build up a compact, large area (246 cm<sup>2</sup>), highly efficient detector system.
- A lightweight cryogenic target (sidewall thickness between 140 to 180  $\mu\text{m}$  made of 2 layers of 50  $\mu\text{m}$  Kapton glued together with an epoxy adhesive) with a working temperature of 30 K and a maximum working pressure of 0.3 MPa, allowing for an x-ray transmission of approximately 90% for 8 keV x-rays.
- A veto system, consisting of an outer veto detector (Veto-1) as active shielding and an inner veto detector (Veto-2) for the suppression of charged particles. Additionally, for both veto systems an excellent time resolution is required to distinguish between kaons stopped in gas and kaons stopped in the target entrance window or sidewall. MC studies require the time resolution of the veto devices to be better than 500 ps (Full Width Half Maximum, FWHM).

For SIDDHARTA-2, an improvement of the signal to background ratio of at least one order of magnitude as compared to the  $K^-p$  measurement of SIDDHARTA is crucial. Firstly, the yield of the  $K^-d$  x-rays is an order of magnitude lower in comparison to kaonic hydrogen as a result of the possibility of two-nucleon-absorption in kaonic deuterium. Secondly, theoretical predictions of the  $1s$  ground state width are in the order of 800 to 1000 eV, approximately larger than in the  $K^-p$  case by a factor of two [7].

Therefore, one of the necessary improvements is the Veto-2 system, which will suppress the beam-correlated background originating from minimum ionizing particles (MIPs, mostly protons and pions) accompanying the x-ray signals. Depending on the position of the MIP passing the SDD, a signal mimicking an x-ray event can be produced. Thus, the charged particle suppression will

be based on the determination of the spatial correlation between a signal in the SDD and a Veto-2 signal.

## 2. Experimental Setup

The SIDDHARTA-2 setup is shown in figure 1. Passing the beam pipe, degrader, kaon trigger, entrance window of the vacuum chamber and target window, the  $K^-$  will enter the cryogenic target cell and be stopped in gaseous deuterium. The target cell will be made of two glued layers of  $50\ \mu\text{m}$  Kapton with a diameter of 144 mm and height of 130 mm and will be surrounded by 48 SDD arrays, resulting in 384 readout channels. The SDDs will be surrounded by the two veto detector systems.

In order to determine the position of the MIPs traversing the SDDs, the Veto-2 system will be mounted directly behind the x-ray detectors (figure 2). The size of the scintillator tiles is optimised to reduce the MIPs-associated background by at least a factor of two, while keeping the losses of good x-ray signals below 10% [5]. The other veto system, consisting of an outer ring of scintillator panels, will act as active shielding.

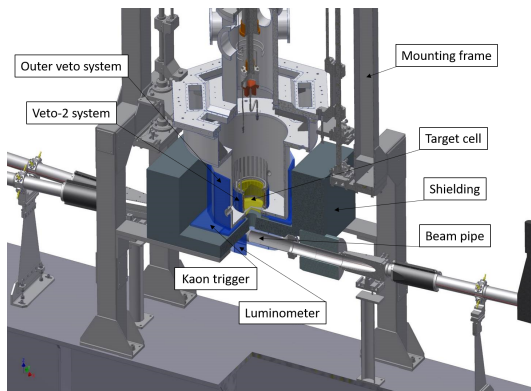


**Figure 1.** Schematic setup of SIDDHARTA-2: Beam pipe, kaon trigger system, target cell, veto systems and mounting frame

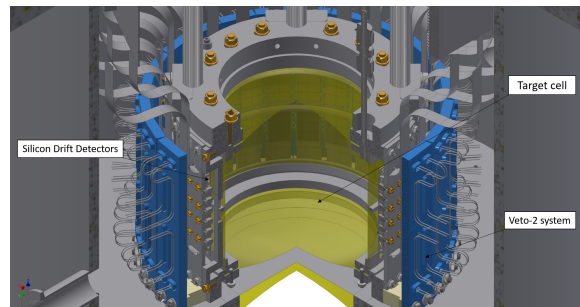


**Figure 2.** Cryogenic target cell (yellow) surrounded by the SDDs and the charged particle veto system (blue)

## 3. The Veto-2 System

The Veto-2 system consists of 96 plastic scintillator tiles (Scionix Holland EJ-200) of size  $50 \times 12 \times 4\ \text{mm}^3$ , with one Silicon PhotoMultiplier (SiPM) manufactured by AdvanSiD attached to the short side of each scintillator. The SiPMs operate in the near-UV region with their maximum photo detection efficiency at 420 nm, featuring an active area of  $4 \times 4\ \text{mm}^2$ . A clear two-component epoxy adhesive (EPO-TEK<sup>®</sup> 301) is used for gluing the SiPMs to the scintillators.

The cable length between the SiPM and the amplifier usually plays a crucial role by influencing the time resolution and leading to an increase of the pick-up noise. Different lengths of twisted pair cables were tested with the dedicated readout electronics. It was concluded that a cable as long as 125 cm can be used without influencing the performance of the SiPMs, which is necessary for the final SIDDHARTA-2 setup.

The scintillator tiles with attached SiPMs are placed in 24 black, 3D-printed boxes, with one of them shown in figure 3. Each box contains four detectors separated by a Teflon layer to avoid cross talk between the scintillator tiles. For a permanent light-tight closure of the boxes, black

epoxy adhesive (Aremco-Bond 2310) is used. The 24 housing panels will be adjusted around an aluminium mounting ring. For the amplification of the SiPM signal, dedicated boards developed at SMI with 12 pairs of analog and digital channels are used. The digital output provides a Time-over-Threshold (ToT) LVDS signal, thus allowing for an increase in cable length of up to 10 m of simple twisted-pair cables to the data acquisition system (DAQ).

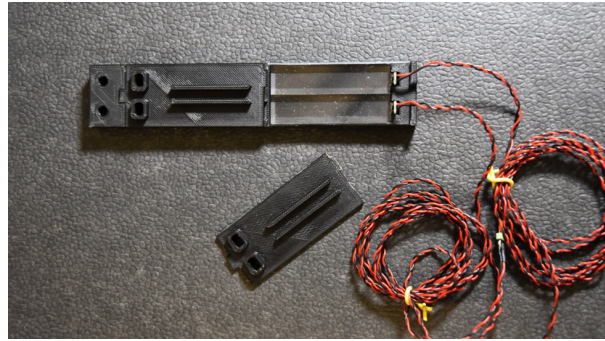


**Figure 3.** Housing unit containing two scintillator-SiPM tiles

### 3.1. The SiPM readout electronics

The Intelligent Front-end Electronics for Silicon photo detectors (IFES) was developed at Stefan Meyer Institute for the operation of SiPMs. These IFES modules feature a feedback loop controlled constant current source based on a boost-converter. The readout of the detector provides both an amplified analog signal in the form of a differential signal and a Low Voltage Differential Signal (LVDS) for the digital output, delivering a time-over-threshold (ToT) pulse with a remotely adjustable threshold. The design of the system enables the operation of larger detector arrays with simple remote control of the comparator threshold and the current source for biasing the SiPM. The block diagram of the IFES modules is shown in figure 4.

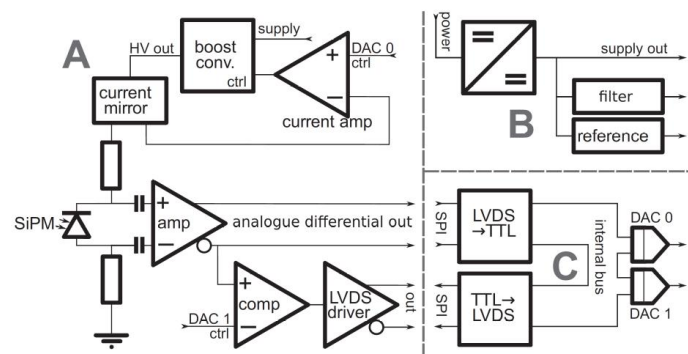


**Figure 4.** IFES block diagram. (A) Detector bias, differential amplifier and comparator, with the signal production within the detector (SiPM). (B) Power supply with filter and reference voltage. (C) Control bus with daisy chain capability and DAC connections [8]

## 4. First Test Results

### 4.1. Time Resolution

The time resolution of the scintillator-SiPM tiles was examined by using a pulsed diode laser with a wavelength of 450 nm as probing radiation. The laser pulse amplitude (4.2 V) and

width (2.8 ns) were chosen in a way that the jitter of the laser pulse was minimised, which, without beam splitter or attenuation, leads to an operation of the SiPM-amplifier combination in saturation. The saturation mode provides the advantage of a faster rise time of the output signal with less jitter, allowing to achieve satisfying results with a simple threshold trigger, by measuring the time delay between the laser pulse and the signal of the SiPM.

This simple test setup was used for quality control of the produced scintillator tiles as well as to extract information on the position depending timing resolution.

Three or five different laser incident positions on each scintillator were irradiated in order to study the homogeneity of the timing of the scintillator tiles, as shown in figure 5. Specifically, the three positions aligned along the longitudinal centre of the scintillator were measured each time. The time resolution for each position was determined by applying a Gaussian fit to the data set and calculating the FWHM, with an example being shown in figure 6.

To give an approximation of the time resolution for all SiPM-scintillator tiles, the average of all measured results was calculated and found to be  $(54.0 \pm 0.1_{stat} \pm 2.0_{syst})$  ps. The statistical uncertainty originates from the Gaussian fit and is much smaller compared to the dominating systemic uncertainty which represents the scattering of the data around the mean as shown in figure 7. It can be explained by the possibility of a deviation of the irradiation angle of the laser, irregularities on the surface or inhomogeneously distributed colour collection centres of the scintillators.

Despite the scattering of the data points around the mean in dependence of the irradiation position, figure 8 shows that no systematic trend correlates the measured time resolution and the path length covered by the laser light.

No attempt was made to improve the setup, since the achieved result was already by at least a factor of 9 better than required and in addition shows that the production process of the scintillator tiles is very well under control.

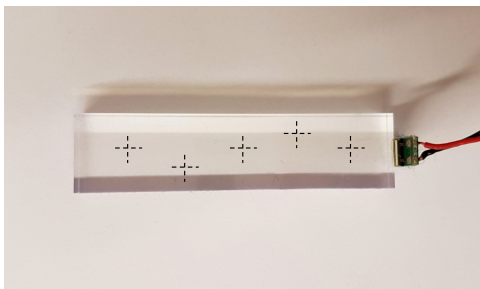


**Figure 5.** Different laser incident positions on the scintillator

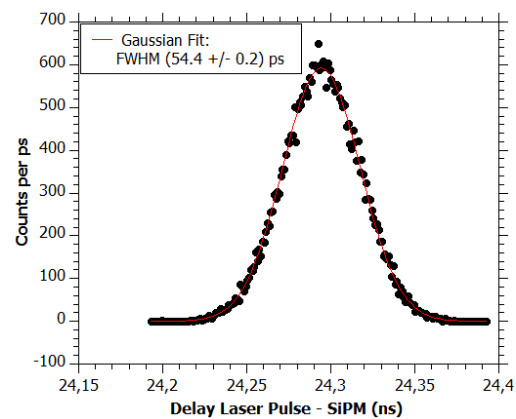


**Figure 6.** Time resolution of one scintillator observed to be  $(54.4 \pm 0.2)$  ps (FWHM) (red: Gaussian Fit)

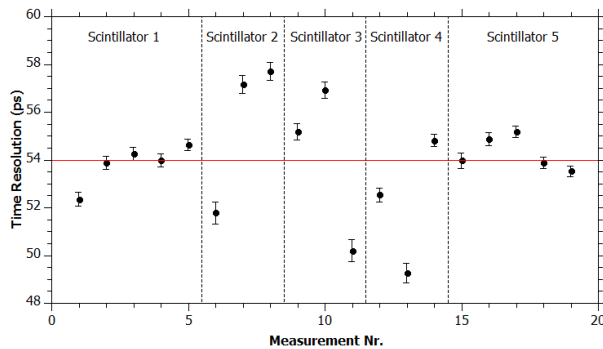


**Figure 7.** Time resolution measurements for five scintillators and total average (red line)

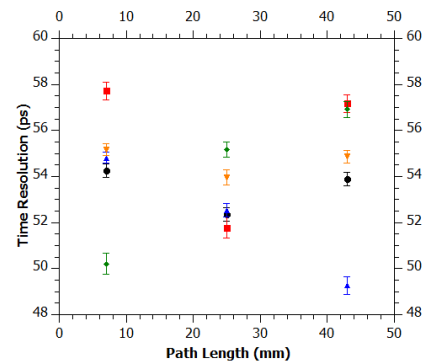


**Figure 8.** Time resolution measurements for different light path lengths measured for five scintillators

#### 4.2. Detection Efficiency

The detection efficiency of the scintillator-SiPM tiles was studied. For this, four scintillators were arranged vertically and cosmic rays were used as radiative source in order to measure the pulse height spectra of all four detector units. Given a coincidence of the outermost detector signals, the abundance of signals of the SiPMs in the middle was determined.

Due to the relatively low rate of cosmic rays passing the stack in this configuration, the measurement acquired data for four days. The observed pulse height distributions are shown in figure 9. For the detectors at the top and bottom positions (SiPM 1 and SiPM 4, respectively), a threshold of 400 mV was set in order to suppress low-energetic background as well as events triggered by cosmic passing the stack in a diagonal way, depositing less energy in the outer scintillators.

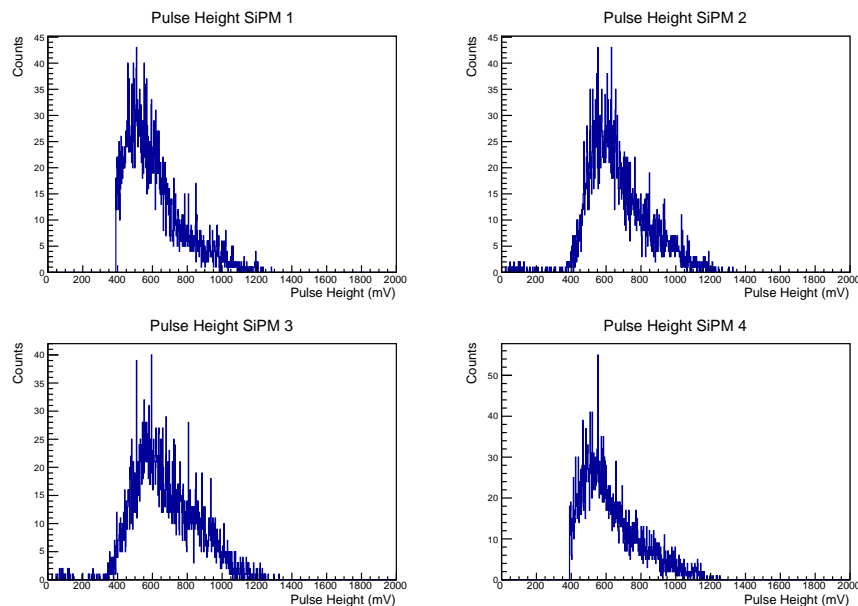


**Figure 9.** Pulse height spectra for the stack of four detector units with a threshold of 400 mV for SiPM 1 positioned at the top and SiPM 4 at the bottom

In order to determine the detection efficiency for SiPM 2 and SiPM 3, only signals above a threshold of 300 mV were taken into consideration. This threshold was chosen in a way to constrain the calculation to cosmic ray events only, while also accounting for the possibility of grazing particle hits due to the scintillators not being aligned perfectly.

In this way, detection efficiencies of  $(99.05 \pm 0.14) \%$  for SiPM 2 and  $(99.14 \pm 0.14) \%$  for SiPM 3 were achieved.

A MC simulation of the cosmic ray spectrum for one of the detectors in the middle of the stack was performed. Figure 10 shows the energy spectrum observed in this measurement and the calculated MC spectrum (red). The simulated spectrum results from muons with normally distributed momenta between 150 and 700 MeV/c. As shown in figure 10, the simulation is overall in good agreement with the obtained cosmic ray data. At lower energies between 650 and 700 keV, the MC calculation does not accurately describe the observed data, because the simple MC simulation does not include the low-energetic part of the cosmic ray spectra. In general, the simulation confirms the observed spectra for SiPM 2 and SiPM 3 (figure 9).

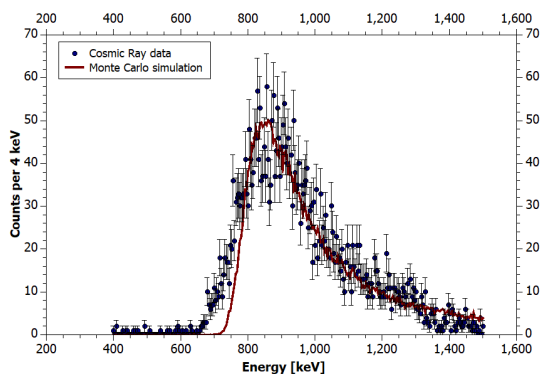


**Figure 10.** MC simulation of an energy spectrum originating from muons with momenta between 50 and 750 MeV/c (red) compared to the observed cosmic ray energy spectrum for SiPM 2

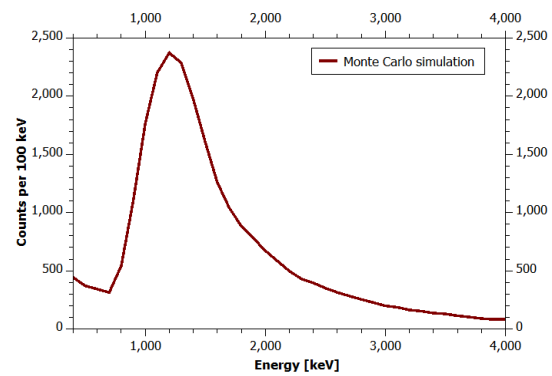


**Figure 11.** MC simulated energy spectrum resulting from expected decay products from antikaon-nucleon reactions at the SIDDHARTA-2 setup

Since under realistic conditions the Veto-2 system will be exposed mainly to MIPs originating from kaon-absorption on the nucleons and not cosmic rays, a dedicated MC simulation with the radiative background expected at SIDDHARTA-2 was performed to compare it with the energy spectra measured using cosmics (figure 11). The  $K^-N$  reaction products taken into consideration are  $\Sigma^\pm\pi^\mp$ ,  $\Sigma^0\pi^0$ ,  $\Lambda\pi^-$ ,  $\Sigma^0\pi^-$  and  $\Sigma^-\pi^0$ , leading to the production of mainly charged pions, protons, neutrons and gammas. Resulting from these particles, the simulated spectrum shows a shift to higher energies in comparison to the cosmic ray data due to the higher energy deposited by the decay products. However, it is expected that this shift will not impact the detection efficiency.

Therefore, it can be concluded that the observed efficiency values provide a reasonable measure for the detection efficiency expected at SIDDHARTA-2.

## 5. Summary and Outlook

The construction of the Veto-2 system has been finished and both severe requirements on efficiency and time resolution have been successfully accomplished with an average time resolution of  $(54 \pm 2)$  ps and detection efficiencies of 99 %.

Further test measurements for the Veto-2 system are planned, mainly to study the correlation between pulse height and time-over-threshold of the SiPMs, since for the final experiment only a multi-hit Time-to-Digital-Converter (CAEN V1190A) will be used and the energy deposit in the scintillator will be determined by the ToT lengths. On-site installation of the SIDDHARTA-2 setup at the LNF is foreseen for autumn 2018 with the commissioning run at DAΦNE being planned for beginning of 2019 and the production beam-time starting in spring 2019.

## Acknowledgments

We thank C. Capocchia, G. Corradi, B. Dulach and D. Tagnani from LNF-INFN; and H. Schneider, L. Stohwasser, D. Pristauz-Telsnigg, V. Kletzl and C. Leeb from Stefan Meyer Institute, for the important contribution in designing and building the SIDDHARTA-2 setup. Part of this work was supported by the Ministero degli Affari Esteri e della Cooperazione Internazionale, Direzione Generale per la Promozione del Sistema Paese (MAECI), Strange Matter project.

## References

- [1] Zmeskal J *et al.* 2015 *Acta Phys. Pol. B* **46** 101
- [2] Bazzi M *et al.* 2011 *Phys. Lett. B* **704** 113
- [3] Mai M and Meißner U G 2013 *Nucl. Phys. A* **900** 51
- [4] Ikeda Y, Hyodo T and Weise W 2011 *Phys. Lett. B* **706** 63
- [5] Cargnelli M, priv. communication
- [6] Berucci, C 2017 *Design and Setup of a High Resolution X-ray Detector System to Study Strong Interaction Induced Width and Shift of the 1s Ground State of Kaonic Deuterium* (PhD thesis) Univ. of Vienna
- [7] Hoshino T *et al.* 2017 *Phys. Rev. C* **96** 045204
- [8] Sauerzopf C *et al.* 2016 *Nucl. Instrum. Meth. Phys. Res. A* **819** 163166